

Samples (50 μL) were taken periodically and filtered through a silica plug to remove the catalyst. The plug was washed with dichloromethane ($3 \times 0.5 \text{ mL}$). The filtrates were combined and analyzed by quantitative GLC analysis (HP-5 column, 5° min^{-1} temperature increase, 50°C initial oven temp, 100°C final temp). The total turnover number was determined as the total concentration of oxidation products (styrene oxide (ca. 92%) and phenylacetaldehyde (ca. 8%)) divided by the initial catalyst concentration.

The epoxidation selectivity experiments were conducted as follows: MnDPyP (3 μmol , 1 equiv) and $[\text{Re}(\text{ZnDPyP})]_4$ (1 equiv) were dissolved in dichloromethane (3 mL) followed by the addition of modifying ligands (30–300 equiv). *cis*-Stilbene (100 equiv) and **5** or **6** (100 equiv) were added to the mixture. PhIO (100 equiv) was then added. Samples (250 μL) were taken after 10, 20, and 30 min, passed through a neutral alumina plug with pentane eluent (15 mL), and analyzed by HPLC (nitrile column eluted with hexanes). Selectivity is defined as $[\text{cis-stilbene oxide} + \text{trans-stilbene oxide}] / [\text{sum of epoxides from } \mathbf{5} \text{ or } \mathbf{6}]$ and normalized against MnDPyP.

Received: June 27, 2001 [Z17375]

- [1] We emphasize, however, that processes other than epoxidation could equally well have been targeted for study. See for example: M. Nakash, Z. Clyde-Watson, N. Feeder, J. E. Davies, S. J. Teat, J. K. M. Sanders, *J. Am. Chem. Soc.* **2000**, *122*, 5286–5293, and references therein.
- [2] M. O. Senge, C. J. Medforth, T. P. Forsyth, D. A. Lee, M. M. Olmstead, W. Jentzen, R. K. Pandey, J. A. Shelnutt, K. M. Smith, *Inorg. Chem.* **1997**, *36*, 1149–1163.
- [3] A. D. Adler, F. R. Longo, F. Kampas, J. Kim, *J. Inorg. Nucl. Chem.* **1970**, *32*, 2443–2445.
- [4] R. L. Halterman in *Transition Metals in Organic Synthesis*, Vol. 2 (Eds.: M. Beller, C. Bolm), Wiley-VCH, Weinheim, **1998**, pp. 300–306.
- [5] L. A. Campbell, T. Kodadek, *J. Mol. Catal. A* **1996**, *113*, 293–310.
- [6] A. M. D. R. Gonsalves, M. M. Pereira, *J. Mol. Catal. A* **1996**, *113*, 209–221, and references therein.
- [7] M. J. Guther, P. Turner, *Coord. Chem. Rev.* **1991**, *108*, 115–161.
- [8] M. L. Merlau, W. J. Grande, S. T. Nguyen, J. T. Hupp, *J. Mol. Catal. A* **2000**, *156*, 79–84.
- [9] For related reports on noncatalytic directed assembly, see for example: M. D. Levin, P. J. Stang, *J. Am. Chem. Soc.* **2000**, *122*, 7428–7429; B. Olenyuk, J. A. Whiteford, A. Fechtenkotter, P. J. Stang, *Nature* **1999**, *398*, 796–799; S. Leininger, B. Olenyuk, P. J. Stang, *Chem. Rev.* **2000**, *100*, 853–907; N. Takeda, K. Umemoto, K. Yamaguchi, M. Fujita, *Nature* **1999**, *398*, 794–796; P. J. Stang, B. Olenyuk, *Coord. Chem. Rev.* **1997**, *30*, 502–518.
- [10] For selected examples, see J. P. Collman, V. J. Lee, C. J. Kellen-Yuen, X. Zhang, J. A. Ibers, J. I. Brauman, *J. Am. Chem. Soc.* **1995**, *117*, 692–703; K. Konishi, K.-I. Oda, K. Nishida, T. Aida, S. Inoue, *J. Am. Chem. Soc.* **1992**, *114*, 1313–1317; E. Rose, A. Kossanyi, M. Quelquejeu, M. Soleilhavoup, F. Duwauran, N. Bernard, A. Lécas, *J. Am. Chem. Soc.* **1996**, *118*, 1567–1568; Y. Naruta, F. Tani, N. Ishihara, K. Maruyama, *J. Am. Chem. Soc.* **1991**, *113*, 6865–6872; D. K. Smith, F. Diederich, *Top. Curr. Chem.* **2000**, *210*, 183–227.
- [11] R. V. Slone, J. T. Hupp, *Inorg. Chem.* **1997**, *36*, 5422–5423.
- [12] Binding constants were determined by UV/Vis titrimetric methods using the Soret band shift of zinc porphyrins upon coordination of nitrogen bases as an indicator.
- [13] Variable substrate (styrene) concentration experiments with catalyst assembly [**1+2**] reveal there is Michaelis–Menten kinetic behavior, with values of about 1 M for the phenomenological Michaelis constant K_m and about 46 s^{-1} for the kinetic constant k_{cat} .
- [14] M. H. Keefe, R. V. Slone, J. T. Hupp, K. F. Czaplewski, R. Q. Snurr, C. L. Stern, *Langmuir* **2000**, *16*, 3964–3970.
- [15] Control experiments using *fac*- $[\text{Re}(\text{CO})_3(\text{pyridine})_2\text{Cl}]$ (a surrogate for the corner structures of the square, **2**), ZnDPyP, or H_2DPyP with styrene and iodosylbenzene gave no detectable epoxidation products.
- [16] The rate of catalysis with the supramolecular assembly, however, was a factor of three slower than for the naked catalyst. Electronic effects are unlikely to account for the difference, since the strength of the coordination bonds linking **1** to **2** are comparatively weak and since the pyridine groups used by the catalyst to drive directed-assembly are

almost certainly oriented out-of-plane with respect to the catalyst's metalloporphyrin core. We tentatively ascribe the rate decrease instead to hindered transport of reactants into the encapsulated active site.

- [17] Turnover numbers are approximately 65 for free catalyst **3** (similar to **1**).
- [18] C. H. Kirksey, P. Hambright, C. B. Storm, *Inorg. Chem.* **1969**, *8*, 2141–2144.
- [19] M. Nappa, J. S. Valentine, *J. Am. Chem. Soc.* **1978**, *100*, 5075–5080.
- [20] S. Belanger, J. T. Hupp, *Angew. Chem.* **1999**, *111*, 2360–2362; *Angew. Chem. Int. Ed.* **1999**, *38*, 2222–2224.
- [21] S. Belanger, J. T. Hupp, C. L. Stern, R. V. Slone, D. F. Watson, T. G. Carrell, *J. Am. Chem. Soc.* **1999**, *121*, 557–563.
- [22] S. Belanger, K. J. Stevenson, S. A. Mudakha, J. T. Hupp, *Langmuir* **1999**, *15*, 837–843.
- [23] J. R. Cupp-Vickery, T. L. Poulos, *Nat. Struct. Biol.* **1995**, *2*, 144. Structure obtained from the Protein Database ID: 1OXA.

A Three-Dimensional Ferrimagnet with a High Magnetic Transition Temperature (T_C) of 53 K Based on a Chiral Molecule**

Katsuya Inoue,* Hiroyuki Imai, Prasanna S. Ghalsasi, Koichi Kikuchi, Masaaki Ohba, Hisashi Ōkawa, and J. V. Yakhmi

Investigation of molecule-based magnets, which began in the late 1960s, has led to the successful synthesis of room temperature magnets.^[1] Specific features considered in molecule-based magnets include: 1) the ability to design the magnet as well as its structural dimensionality, 2) magnet solubility in water or organic solvents, and, 3) the optical transparency of the magnet.^[2] The physical characteristics of greatest interest are the optical properties, particularly with respect to natural optical activity. On the basis of theoretical calculations, new phenomena were expected in optically active magnetic materials.^[3] In 1997, Rikken and Raupach observed a small magneto-chiral dichroism (MChD) effect in a chiral paramagnetic material.^[4] This effect depends on the

- [*] Prof. Dr. K. Inoue, Dr. H. Imai
Department of Applied Molecular Science
Institute for Molecular Science, Okazaki 444-8585 (Japan)
Fax: (+81) 564-54-2254
E-mail: kino@ims.ac.jp
- Dr. P. S. Ghalsasi
University of Mumbai, Department of Chemical Technology
Mumbai, 400019 (India)
- Prof. Dr. K. Kikuchi
Department of Chemistry, Tokyo Metropolitan University
Hachioji, Tokyo 192-0367 (Japan)
- Dr. M. Ohba, Prof. Dr. H. Ōkawa
Department of Chemistry, Graduate School of Science
Kyusyu University, Fukuoka 812-8581 (Japan)
- Prof. Dr. J. V. Yakhmi
Chemistry Division, Bhabha Atomic Research Center
Mumbai, 400085 (India)

[**] This work was supported by a program entitled “Research for the Future (RFTF)” of the Japan Society for the Promotion of Science (99P01201).

magnetization of the material, and relatively large effects are expected in the chiral magnets relative to paramagnetic materials. When we construct magnets based on chiral molecules, the chirality must be controlled not only in the molecular structure, but in the entire crystal structure as well. As a consequence of this difficulty few examples of this type of magnet exist.^[5, 6]

We have introduced a strategy of using π -conjugated high-spin oligonitroxide radicals as bridging ligands for paramagnetic transition metal ions in order to assemble and align electron spins on a macroscopic scale.^[5, 7] In fact, we have succeeded in synthesizing the first chiral magnet by this strategy.^[5] These bisnitroxide- or nitronitroxide-manganese-based systems are one-dimensional, consequently the transition temperatures required to produce a magnet were low. On the other hand, cyano-bridged dimetallic three-dimensional complexes (Prussian-Blue family) are well known to be promising candidates for producing high transition temperature (T_C) magnetic materials with spontaneous magnetization.^[8] Here we report on the crystal structure and physical properties of a 3D chiral ferrimagnet, $K_{0.4}[Cr(CN)_6][Mn(S)\text{-pn}](S)\text{-pn}H_{0.6}$ ((*S*)-pn = (*S*)-1,2-diaminopropane).

The complex $K_{0.4}[Cr(CN)_6][Mn(S)\text{-pn}](S)\text{-pn}H_{0.6}$ was obtained as pale yellow needle crystals by the reaction of $K_3[Cr(CN)_6]$, $Mn(ClO_4)_2$, and (*S*)-1,2-diaminopropane dihydrochloride ((*S*)-pn \cdot 2HCl) in a 2:3:3 molar ratio in a mixture of methanol and H_2O (1/1; adjusted to pH 7–8 by KOH) under an argon atmosphere. An X-ray structural analysis of a hexagonal crystal of the complex revealed the formation of the chiral 3D network (Figures 1 and 2).^[9] In contrast to $[Mn(en)]_3[Cr(CN)_6]_2 \cdot 4H_2O$, only four cyanide groups in the $[Cr(CN)_6]^{3-}$ ion are ligated to Mn^{2+} ions to form the helical dimetallic loops along the *c* axis and to connect the adjacent

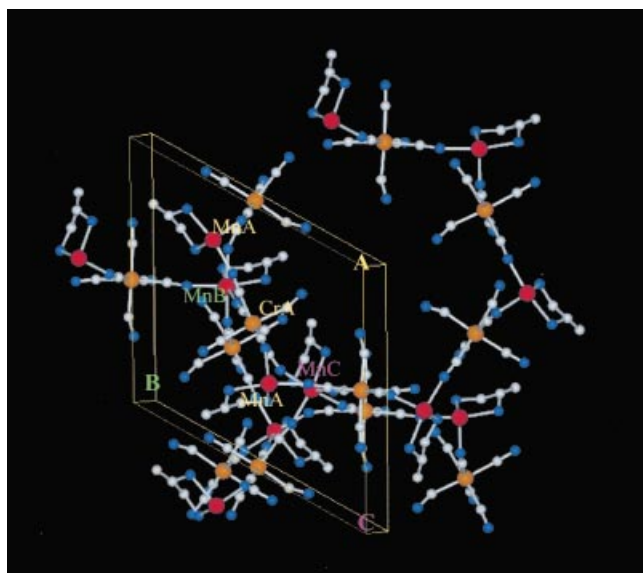


Figure 1. Crystal structure of $K_{0.4}[Cr(CN)_6][Mn(S)\text{-pn}](S)\text{-pn}H_{0.6}$. Views along the *c* axis (A) and of the connection of helical dimetallic loops (B). Some atoms are omitted for clarity. Color scheme: Cr: brown, Mn: red, C: gray, N: blue. CrA in loop A is connected not only to MnA and MnA' in loop A, but also to MnB and MnC in loops B and C, respectively.

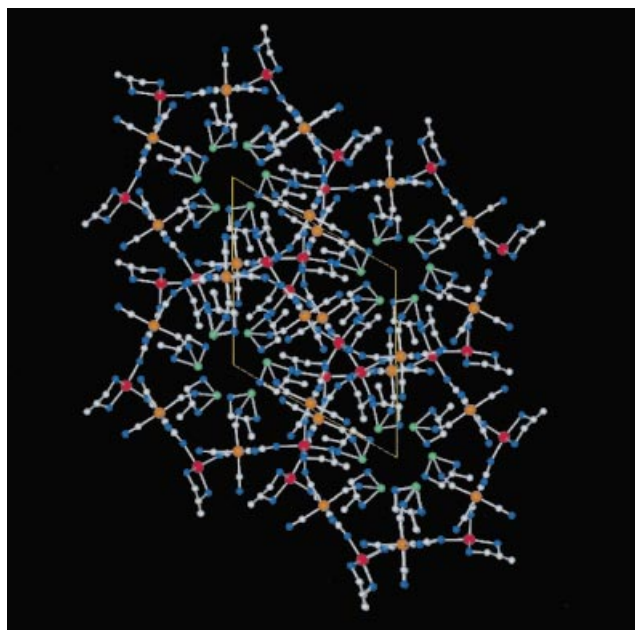


Figure 2. Crystal structure of $K_{0.4}[Cr(CN)_6][Mn(S)\text{-pn}](S)\text{-pn}H_{0.6}$. Views along the *c* axis and showing the connection of the helical dimetallic loops. The same color scheme is used as in Figure 1 and with K atoms shown in green.

loops. The Cr...Mn distances (CrA...MnA: 5.21 and CrA...MnA': 5.28 Å) within a loop are a little shorter than those (CrA...MnB: 5.39 and CrA...MnC: 5.32 Å) between loops. A single unit possesses two chiral ligands of (*S*)-pn; one is coordinated to a Mn^{2+} ion and the other is located in the cavity of the helical loop and partially coordinated to the K^+ counterion. The site occupancy of the K^+ ion is not unity but 0.4, so about 60% of the latter (*S*)-pn ligand may be protonated to become (*S*)-pnH⁺ ions so as to maintain overall neutrality.^[10]

The magnetic behavior of the complex was measured on a SQUID susceptometer in the temperature range of 2–300 K and the magnetic field range of 0–5 T. The temperature dependence of the magnetic susceptibility is shown in Figure 3. The $\chi_{mol}T$ value is 4.88 emu K mol^{−1} (6.25 μ_B) at 300 K and decreases with decreasing temperature down to a minimum value of 3.66 emu K mol^{−1} (5.41 μ_B) at 110 K. The

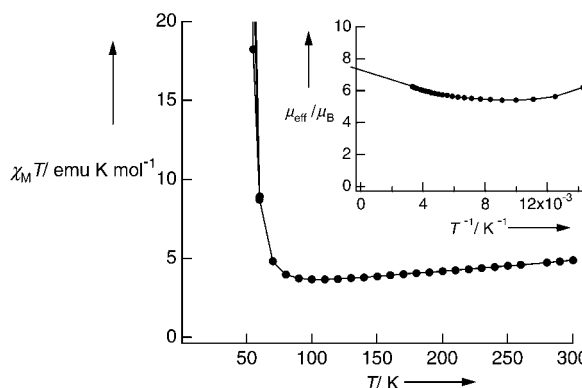


Figure 3. Temperature dependence of $\chi_{mol}T$ values of $K_{0.4}[Cr(CN)_6][Mn(S)\text{-pn}](S)\text{-pn}H_{0.6}$ in the magnetic field of 5000 Oe. Inset: Plot of effective magnetic moment versus $1/T$.

extrapolated effective magnetic moment value of $7.2 \mu_B$ is in good agreement with the theoretical value at the high temperature limit (Figure 3 inset; calculated with a paramagnetic spin of $5/2 + 3/2 \rightarrow 7.07 \mu_B$). Upon further cooling the sample, the $\chi_{\text{mol}}T$ value increases and diverges. A plot of $1/\chi_{\text{mol}}$ versus T in the range from 300 to 110 K obeys the Curie–Weiss law with a Weiss temperature $\theta = -30.9$ K. This value indicates that the antiferromagnetic interaction operates between adjacent Cr^{3+} and Mn^{2+} ions through the cyanide bridges above 110 K. The abrupt increase in the $\chi_{\text{mol}}T$ value around 60 K suggests the onset of three-dimensional magnetic ordering.

Both the field cooled (FC) and the zero field cooled (ZFC) magnetization measurements (ZFC) with a low applied field (5 G) in the temperature range from 5 to 100 K show a long-range magnetic ordering below 53 K (Figure 4). The magnetization (M) increases sharply with the applied field and is

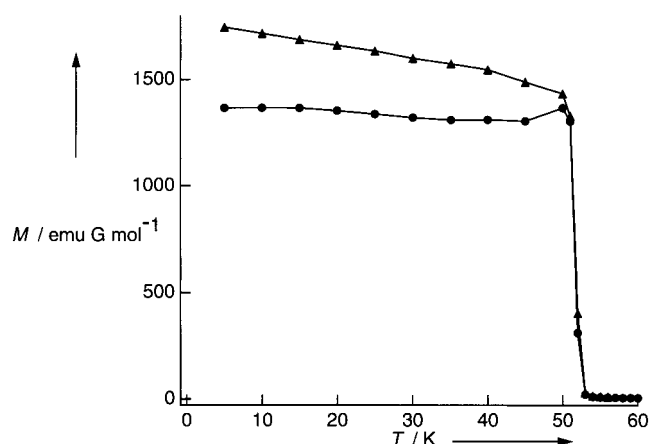


Figure 4. Temperature dependence of the magnetization of $\text{K}_{0.4}[\text{Cr}(\text{CN})_6][\text{Mn}(\text{S})\text{-pn}](\text{S})\text{-pnH}_{0.6}$. The FC (\blacktriangle) and ZFC (\bullet) magnetization measurements are shown.

saturated rapidly (Figure 5). The saturation magnetization (M_s) is $2 \mu_B$. This value is in good agreement with the theoretical value of antiferromagnetic coupling between Cr^{3+} and Mn^{2+} ions ($5/2 - 3/2 = 2/2$). The magnetic hysteresis

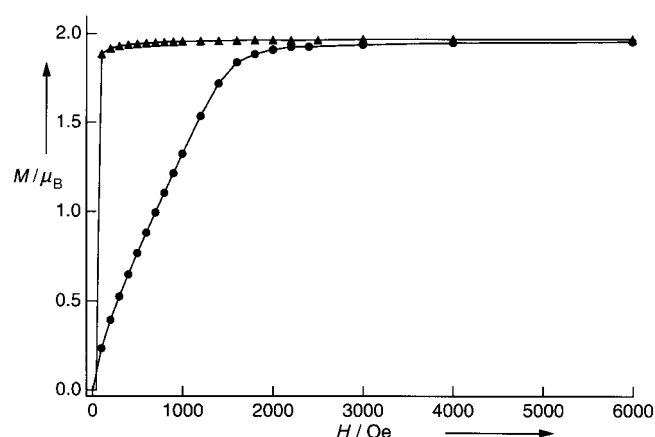


Figure 5. Field dependence of the magnetization at 5 K along the easy axis (c axis, \blacktriangle) and the hard axis (perpendicular to c axis; \bullet).

loop (the remnant magnetization of $30 \text{ emu G mol}^{-1}$ and the coercive field of 12 Oe) was observed at 2 K, which shows there is a soft magnetic behavior.

In summary, we have successfully constructed the first novel 3D, fully chiral ferrimagnet; moreover, this ferrimagnet was characterized structurally. Further, the magnetic transition temperature of this complex is relatively high (53 K) for a molecule-based magnet. We believe that this complex is a potential candidate for novel magneto-optical phenomena. In addition to this complex, we have already obtained a few crystals of 3D chiral magnets based on a polymeric cyano-bridged Cr^{3+} - Mn^{2+} compound. It is hoped that these complexes will subsequently lead to the development of a novel group of molecule-based magnets.

Experimental Section

A solution of $(S)\text{-pn} \cdot \text{HCl}$ (0.1 mmol) in water (1 mL) was adjusted to pH 7–8 by the addition of a solution of KOH (0.12 mmol) in water (0.3 mL). A solution of $\text{Mn}(\text{ClO}_4)_2 \cdot 6\text{H}_2\text{O}$ (0.1 mmol) in water (0.8 mL) was added to the $(S)\text{-pn}$ solution under an argon atmosphere. A glass tube (ca. 8 mm diameter, ca. 20 cm long) was charged with this $(S)\text{-pn}$ and manganese solution, and a mixture of methanol and H_2O (1/2, 1.5 mL) was gently added as an upper layer. A solution of $\text{K}_3[\text{Cr}(\text{CN})_6]$ (0.07 mmol) in methanol/ H_2O (1/1, 1 mL) was added carefully as a third layer under an argon atmosphere, and then the tube sealed. Crystals of the $\text{K}_{0.4}[\text{Cr}(\text{CN})_6][\text{Mn}(\text{S})\text{-pn}](\text{S})\text{-pnH}_{0.6}$ complex grew as pale yellow needles after several weeks.

Received: June 27, 2001 [Z17372]

- [1] J. M. Manriquez, G. T. Yee, R. S. Mclean, A. J. Epstein, J. S. Miller, *Science* **1991**, 252, 1415; S. Ferlay, T. Mallah, R. Ouahés, P. Veillet, M. Verdaguer, *Nature* **1995**, 378, 701.
- [2] C. Bellitto, P. Day, *J. Chem. Soc. Chem. Commun.* **1978**, 511; "Supramolecular Engineering of Synthetic Metallic Materials Conductors and Magnets": P. Day, *NATO ASI Ser. Ser. C* **1999**, 518, 253.
- [3] G. Wagniere, A. Mejer, *Chem. Phys. Lett.* **1984**, 110, 546.
- [4] G. L. J. A. Rikken, E. Raupach, *Nature* **1997**, 390, 493.
- [5] H. Kumagai, K. Inoue, *Angew. Chem.* **1999**, 111, 1694; *Angew. Chem. Int. Ed.* **1999**, 38, 1601.
- [6] A. Caneschi, D. Gatteschi, P. Ray, R. Sessoli, *Inorg. Chem.* **1991**, 30, 3936; M. Hernández-Molina, F. Lloret, C. Ruiz-Pérez, M. Julve, *Inorg. Chem.* **1998**, 37, 4131; M. Verdaguer, paper presented at the Indo-French Workshop on *Current Trends in Molecular Magnetism* (Bangalore, India), **2000**; E. Coronado, J. R. Galan-Mascaros, C. J. Gomez-Garcia, J. M. Martinez-Agudo, *Inorg. Chem.* **2001**, 40, 113.
- [7] K. Inoue, H. Iwamura, N. Koga, *New J. Chem.* **1998**, 22, 201; K. Inoue, H. Iwamura, *J. Am. Chem. Soc.* **1994**, 116, 3173; A. S. Markosyan, T. Hayamizu, K. Inoue, H. Iwamura, *J. Phys. Condens. Mater.* **1998**, 10, 2323.
- [8] M. Ohba, N. Usuki, N. Fukita, H. Okawa, *Angew. Chem.* **1999**, 111, 1911; *Angew. Chem. Int. Ed.* **1999**, 38, 1795.
- [9] Crystal data for $\text{K}_{0.4}[\text{Cr}(\text{CN})_6][\text{Mn}(\text{S})\text{-pn}](\text{S})\text{-pnH}_{0.6}$: yellow needles, $\text{C}_{12}\text{H}_{20.6}\text{CrK}_{0.4}\text{N}_{10}$. $M_r = 397.8877$, crystal dimensions $0.2 \times 0.15 \times 0.10$ mm, hexagonal, space group $P6_1$, $a = 14.7672(4)$, $c = 17.5731(7)$ Å, $V = 3318.75(18)$ Å³, $\rho_{\text{calcd}} = 1.282 \text{ g cm}^{-3}$, $Z = 6$, $\mu(\text{MoK}\alpha) = 1.282 \text{ mm}^{-1}$. Data were collected on a Bruker SMART-APEX three-circle diffractometer equipped with a CCD area detector (graphite-monochromated $\text{MoK}\alpha$, $\lambda = 0.71073$ Å, ω -scan mode (0.3° steps), semi-empirical absorption correction on Laue equivalents). The structure was solved by direct methods and refined by full-matrix least-squares refinement against F^2 on all data by using SHELXTL software. Hydrogen atoms were included in their calculated positions but not refined. All non-H atoms, except for C and N atoms in $(S)\text{-pn}$ that are located in the hole of the helical loop, were refined

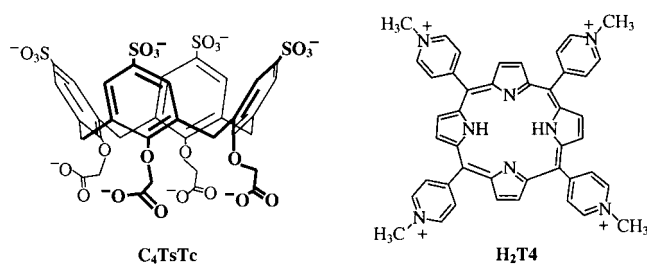
anisotropically. Some disorder in one of the cyanide groups and the (S)-pn ligands coordinated to Mn^{2+} ions was also observed. The occupancy of the disordered atoms and the K^+ ion was determined by population analysis. The refinement converges with $R_1 = 0.0615$ for 2520 data ($I > 4\sigma(I)$), $wR_2 = 0.1371$ for 5405 unique data ($2.81 \leq \theta \leq 28.33^\circ$), Flack parameter = 0.06(5), max/min residual electron density 0.527/−0.298 $\text{e} \text{ \AA}^{-3}$. Crystallographic data (excluding structure factors) for the structure reported in this paper have been deposited with the Cambridge Crystallographic Data Centre as supplementary publication no. CCDC-165941. Copies of the data can be obtained free of charge on application to CCDC, 12 Union Road, Cambridge CB21EZ, UK (fax: (+44) 1223-336-033; e-mail: deposit@ccdc.cam.ac.uk).

Calixarene – Porphyrin Supramolecular Complexes: pH-Tuning of the Complex Stoichiometry**

Luigi Di Costanzo, Silvano Geremia, Lucio Randaccio,* Roberto Purrello,* Rosaria Lauceri, Domenico Sciotto,* Fabio Giuseppe Gulino, and Vincenzo Pavone

The rich chemistry of calixarenes and porphyrins as (polytopic) receptors and photoactive species, respectively, as well as the enormous possibility of functionalizing the periphery of these molecules have boosted the synthesis of their covalent conjugates for use as possible molecular devices.^[1] It has recently been shown, for example, that covalent porphyrin–calixarene conjugates behave as molecular tweezers when individual specific functions are synergistically exploited.^[2] Some preliminary data on the formation of noncovalent complexes have also been reported but, to date, no structural data on such supramolecular species have been presented.^[3]

Here we present a spectroscopic and structural study that shows that the cationic porphyrin ($\text{H}_2\text{T4}$) and the anionic sulphonated calixarene (C_4TsTc) blocked in a *cone* conformation and bearing carboxylic functions^[4] form quite stable supramolecular complexes, both in the solid state and in



aqueous solution. Furthermore, the $\text{H}_2\text{T4}:\text{C}_4\text{TsTc}$ molar ratio is tuned by the protonation state of the C_4TsTc carboxylate groups.

The absorption and fluorescence spectra of $\text{H}_2\text{T4}$ are characterized by an intense absorption band at 422 nm (Soret band) and an emission at 650 nm, respectively. C_4TsTc absorbs in the far UV region (about 200 nm) and, at pH 6, emits at 307 and 602 nm. However, at pH 2.2, where the four carboxylic groups of C_4TsTc are all protonated ($\text{pK}_{\text{a}1} = 3.03$, $\text{pK}_{\text{a}2} = 3.27$, $\text{pK}_{\text{a}3} = 3.97$, $\text{pK}_{\text{a}4} = 4.57$),^[5] the emissions are almost completely quenched.

The interaction of $\text{H}_2\text{T4}$ with C_4TsTc at pH 6 and $I = 0.05 \text{ M}$ (NaCl) is accompanied by significant hypochromism and broadening of the Soret band (see inset of Figure 1) and remarkable quenching of both the porphyrin and calixarene emissions. The spectroscopic features of $\text{H}_2\text{T4}$ at pH 2.2 following complex formation with C_4TsTc ($I = 0.05 \text{ M}$) are very similar to those observed at pH 6.

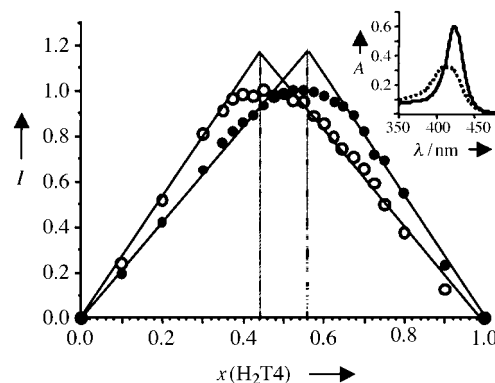


Figure 1. Normalized absorption Job plots at pH 2.2 (○) and 6 (●). The inset shows the absorption spectrum of $\text{H}_2\text{T4}$ (2.8 μM) before (—) and after (---) the addition of C_4TsTc (2.2 μM).

However, the Job plots performed at pH 2.2 and 6 show there is a large difference in the ratio of the complex formed (Figure 1). The maximum value at a porphyrin molar fraction of 0.44 at pH 2.2 indicates the formation of species with a 4:3 $\text{C}_4\text{TsTc}:\text{H}_2\text{T4}$ ratio, whereas the maximum value at a porphyrin molar fraction of 0.56 at pH 6 indicates the formation of species with a 4:5 $\text{C}_4\text{TsTc}:\text{H}_2\text{T4}$ ratio. We were able to obtain single crystals of the porphyrin–calixarene complexes at $\text{pH} \approx 2$ (**1**) and at pH 6 (**2**).

In agreement with the results from the solution study, the $\text{H}_2\text{T4}:(\text{C}_4\text{TsTc}+\text{H}_2\text{T4})$ molar ratio is 0.43 (2 calixarene moieties, 1.5 porphyrin molecules, and 2 sodium ions) in the asymmetric unit of the crystals obtained at $\text{pH} \approx 2$ (**1**).^[6] Here,

[*] Prof. L. Randaccio, Dr. L. Di Costanzo, Dr. S. Geremia
Centro di Eccellenza di Biocristallografia
Dipartimento di Scienze Chimiche, Università di Trieste
via Licio Giorgieri 1, 34127 Trieste (Italy)
E-mail: randaccio@univ.trieste.it

Prof. R. Purrello, Prof. D. Sciotto, Dr. F. G. Gulino
Dipartimento di Scienze Chimiche
Università di Catania
via Andrea Doria 6, 95125 Catania (Italy)
E-mail: rpurrello@dipchi.unict.it, dsciotto@dipchi.unict.it

Dr. R. Lauceri
ISSN, CNR Valverde, Catania (Italy)

Prof. V. Pavone
Dipartimento di Chimica, Università "Federico II"
Complesso Universitario di Monte S. Angelo
via Cynthia 45, 80131 Napoli (Italy)

[**] This work was supported by the Italian MURST (PRIN MM03185591).